LUND UNIVERSITY

Optical porosimetry and investigations of the porosity experienced by light interacting with porous media.

Svensson, Tomas; Alerstam, Erik; Johansson, Jonas; Andersson-Engels, Stefan

Link to publication

Optical porosimetry and investigations of the porosity experienced by light interacting with porous media

Tomas Svensson,[1,*] Erik Alerstam,[1] Jonas Johansson,[2] and Stefan Andersson-Engels[1]

[1]*Department of Physics, Lund University, 221 00 Lund, Sweden*

[2]*Astra Zeneca R&D Mölndal, 431 83 Mölndal, Sweden*
Corresponding author: tomas.svensson@fysik.lth.se

We investigate how light samples disordered porous materials such as ceramics and pharmaceutical materials. By combining photon time-of-flight spectroscopy and sensitive laser-based gas sensing, we obtain information on the extent to which light interacts with solid and pore volumes, respectively. Comparison with mercury intrusion porosimetry shows that light predominantly interacts with the solid. Analysis based on a two-state model does not fully explain observations, revealing a need for refined modeling. Nonetheless, excellent correlation between actual porosity and the porosity experienced by photons demonstrates the potential of nondestructive optical porosimetry based on gas absorption.   © 2010 Optical Society of America

OCIS codes: 120.4290, 300.6500, 300.6320, 290.4210, 160.2710.

Understanding of the interaction of light and turbid porous materials is of fundamental importance in many areas—from fundamental studies of photon localization in porous semiconductor materials [1,2] to analysis of chemistry, pore structure and optics of powders and pharmaceutical materials [3–5], porous ceramics [6–8], and porous silicon [9,10]. Throughout the years, massive efforts have been put into developing models for the macroscopic aspects of photon migration in turbid materials. Radiative transport theory and derivatives (e.g., Monte Carlo simulation and diffusion theory) are the most commonly used models. These models are based on photon conservation, ignore wave properties, and introduce average optical properties to account for microscopic heterogeneity that causes light scattering. Understanding of how photons actually sample turbid heterogenous structures is, however, limited, and the interpretation of average optical properties remains debated.

In this Letter, we report on experimental work aimed at improving fundamental understanding of light propagation in porous materials. We show that photons propagating in porous structures predominantly interact with the solid, and that this phenomenon can be studied in detail by carefully combining photon time-of-flight spectroscopy (PTOFS) and high-resolution gas in scattering media absorption spectroscopy (GASMAS). Our experiments, in combination with mercury intrusion porosimetry (a porosimetry gold standard), provide new insight on the relation between photon travel habits, average optical properties, and material pore structure. In addition, we present a quantitative study of direct optical assessment of porosity. Being based on gas absorption, the method stands in great contrast to work on optical porosimetry based on measurements of light scattering in combination with Mie theory and presupposing negligible material absorption and low porosity [6,7].

Ceramics and stacked crystals are examples of materials with only interparticle porosity, while both interparticle and intraparticle porosity is exhibited by, e.g., zeolite powders and granulated pharmaceutical filler materials. Structure, pore sizes, and porosity strongly influence optical pathlengths and attenuation. In this work,

we assume that light propagation can be described using a two-state model where light at a given time propagates in either solid or pore. The average pathlength through solid, L_s, is of paramount importance, since it determines spectroscopic signatures. Unfortunately, L_s is not easily assessed. Another fundamental question concerns the relation between the material porosity ϕ and the division of the total photon pathlength L in pathlength through the solid, L_s, and pathlength through pore volumes, L_p. In previous work based on PTOFS and GASMAS, it had been assumed that L is divided according to the volume fractions, i.e., $L_s/L = V_s/V$ and $L_p/L = V_p/V$ (where V is the total sample volume and V_s and V_p are the material and pore volume, respectively) [11,12]. Note, however, that the validity of this assumption was questioned already in the first paper, where PTOFS and GASMAS was combined, and further scrutiny was suggested [11]. The present work investigates this important matter and includes studies of photon travel habits in both porous ceramics and complex granulated materials.

PTOFS is employed to determine the photon time-of-flight (TOF) distribution and thus also the average total TOF $t = t_s + t_p$, where t_s and t_p are the time spent in the solid and the pore volume, respectively. Assuming a unitary refractive index in pore volumes, the relation between TOFs and physical pathlengths is

$$L = L_s + L_p = c_0 n_s^{-1} t_s + c_0 t_p, \qquad (1)$$

where c_0 is the speed of light in vacuum and n_s is the refractive index of the solid. To reach deconvoluted information about L_s and L_p, we utilize the absorption exhibited by free gas located in the pores. The spectrally sharp (gigahertz) gas absorption is distinguished from the dull imprints of the solid and is measured by means of GASMAS [13,14]. GASMAS allows measurement of $L_p = c_0 t_p$. Combining GASMAS and PTOFS, L_s can be determined using $L_s = c_0 n_s^{-1} \times (t - t_p)$. GASMAS experiments are conducted by tuning a 0.3 mW vertical-cavity surface-emitting diode laser over the R9Q10 absorption line of molecular oxygen (760.654 nm). A large-area photodiode detects diffuse light transmitted through the

samples. High sensitivity is reached by employing second-harmonic wavelength modulation spectroscopy ($2f$ WMS). The GASMAS setup is described in detail in [12,14]. Note that since we study gas confined in micrometer-sized pores at atmospheric pressure, wall collision broadening (which would appear in nanopores) is negligible [8]. The absorption lineshape of the confined oxygen is therefore the same as free oxygen [see, e.g., Fig. 1(b)]. Our PTOFS experiments are based on picosecond pulsed-light sources, a fast microchannel plate–photomultiplier tube, and time-correlated single-photon counting, allowing measurement of TOF distributions and average absorption and scattering of the material [15,16]. The difference in detector size between GASMAS and PTOFS is taken into account by calculating t for the GASMAS detector using the optical properties derived from PTOFS.

The ceramic material investigated is a macroporous alumina ceramic with a porosity of $\phi_{Hg} = 34.0\%$ and pore diameters mainly in the 1 to 5 μm range (as given by mercury intrusion porosimetry). The sample was made to 92.5% from a 10 μm α-alumina powder (Al_2O_3), the remaining part being a 40 nm silica powder (SiO_2) used as binder. The bulk material was reached by sintering and was polished to a thickness of 2.85 mm (14 mm in diameter). Figure 1 presents experimental data. PTOFS at 760 nm [16] showed that the average total TOF t is 2163 ps, while GASMAS revealed that L_p is 58.8 mm ($t_p = 196$ ps). Since the refractive indexes of α-alumina and silica is 1.765 and 1.5, respectively, n_s can be approximated by 1.75. This means that $L_s = 337.2$ mm and $L = L_s + L_p = 396$ mm. The porosity experienced by photons, $\phi_{opt} = L_p/L$ (from now on termed *optical porosity*), is thus about 14.9%. This data reveal a major discrepancy between optical and actual porosity ($\phi_{opt} = 0.44 \times \phi_{Hg}$).

Turning to complex porous materials with both interparticle and intraparticle porosity, we conducted a detailed study of 12 granulated pharmaceutical tablets with microcrystalline cellulose (MCC) as the main constituent. All had a total weight of 300 mg and were manufactured from two sieve fractions (granule sizes less than 150 μm in group A, and 150–400 μm in group B) using different compression forces (i.e., a subset of the samples described in [12]). The refractive index of the solid material was about 1.5. Photon TOF was measured at 786 nm [12], but the difference in TOF between 786 nm and 760 nm is negligible for these samples (investigated using a tunable instrument [16]). The pore structure was investigated by means of mercury intrusion porosimetry and is presented in Fig. 2. The porosity, ϕ_{Hg}, was between 10% and 30%. Evaluation of PTOFS data [12] yields reduced scattering of $\sim$500 cm^{-1} and absorption of $\sim$0.03 cm^{-1} (varying with compression and granular size). Interestingly, our data again show that ϕ_{opt} significantly deviates from actual porosity. A comparison of optical and actual porosity is given in Fig. 3. Note that simple gravimetric considerations agree with ϕ_{Hg}. The data thus clearly show that photons are predominantly confined to the solid, ϕ_{opt} being $0.48 \times \phi_{Hg}$.

These results show that the use of $\phi_{opt} = L_p/L$ as a measure of porosity, as suggested in previous work combining GASMAS and PTOFS [11,12], can be highly inaccurate. Nonetheless, as shown in Fig. 4, our data give first evidence of an excellent correlation between ϕ_{opt} and ϕ_{Hg}. Since the precision in L_p is better than 2%, and better than 1% for t, the precision in ϕ_{opt} should be $\sim$5% for the samples considered in this work. This shows that our optical approach has a great potential as a tool for rapid and nondestructive porosimetry.

The physical origin of the discrepancy between optical and actual porosity needs further attention. Total internal reflection can potentially explain why photons are predominantly confined to the solid, a phenomenon recently discussed in relation to photon channeling in aqueous foams [17,18]. When geometrical optics is valid, and assuming random angles of incidence and polarization, one can calculate probabilities for photon transfers

Fig. 2. (Color online) Cumulative mercury intrusion for tablets. 1–6 μm pores dominate the pore volume. Compression removes large pores, shifting large-pore cutoff from 5 to 2 μm.
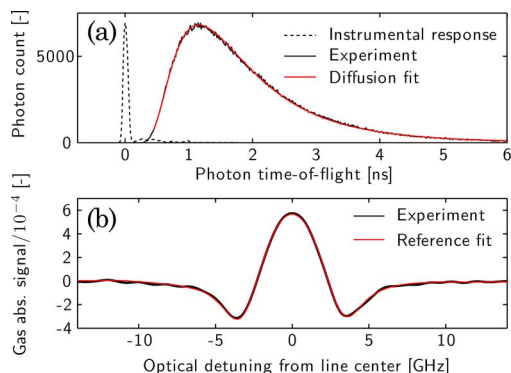

Fig. 1. (Color online) (a) PTOFS and (b) GASMAS data from the macroporous alumina. Diffusion modeling [12] yields a reduced scattering of $\sim$1300 cm^{-1} and negligible absorption. The gas absorption signal is a $2f$ WMS signal. Evaluation using an air spectrum [12] yields a pathlength of 66.0 mm (including a 7.2 mm offset).
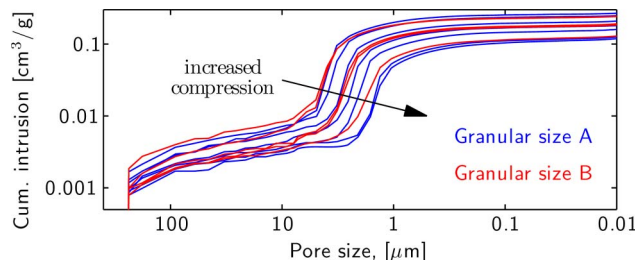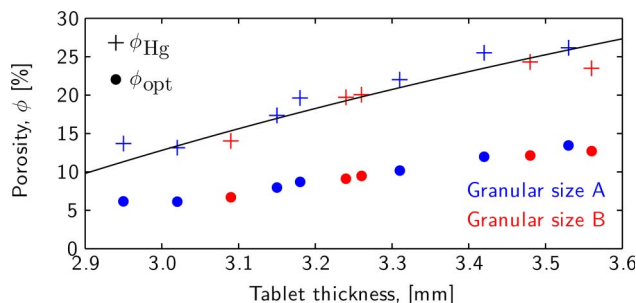

Fig. 3. (Color online) Comparison of optical porosity, ϕ_{opt}, and porosity given by mercury intrusion, ϕ_{Hg}, for 12 pharmaceutical samples. The solid line shows porosity expected from assuming an MCC density of 1.46 g/cm^3. To avoid artifacts due to deformation at high mercury pressures, ϕ_{Hg} is based on the cumulative intrusion at 0.1 μm and may thus be a slight underestimation of the true porosity.
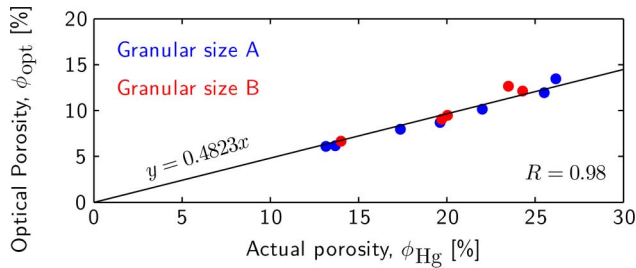
Fig. 4.   (Color online) Correlation between optical and actual porosity (correlation coefficient 0.98, $\phi_{\text{opt}} \simeq 0.48\phi_{\times}\text{Hg}$).

between solid and pore volumes. A simple two-state Markov model can then provide the stationary distribution (fraction of steps in solid, π_s, versus steps in pores, π_p). For the ceramic, $n_s = 1.75$, the probabilities for internal reflection in the solid and pore, respectively, are $p_{ss} = 0.4219$ and $p_{pp} = 0.1166$ (subscripts referring to solid-to-solid and pore-to-pore, respectively). The stationary distribution is then $\pi_s = 0.6044$ and $\pi_p = 0.3956$. Since ϕ and $1 - \phi$ are measures of the relative length of steps in pores and solid compartments, respectively, the optical porosity predicted by this model is

$$\phi_{\text{opt}} = \frac{\pi_p\phi}{\pi_p\phi + \pi_s(1 - \phi)}. \qquad (2)$$

For our ceramic ($\phi = 34\%$) this model suggests that ϕ_{opt} should be about 25%, i.e., 0.74 times the actual porosity. Since our heterogeneities are not much larger than the wavelength, the breakdown of geometrical optics may explain why the observed ratio is as low as 0.44.

For the case of the pharmaceutical samples, where the solid has a lower refractive index, one might expect a smaller difference between ϕ_{opt} and ϕ_{Hg}. Although this agrees with experimental data, the discrepancy between model and experiment remains large. Calculations analogous to those presented above, for $n_s = 1.5$ and ϕ between 10% and 30%, yields optical porosities between 7% and 22% and ratios between 0.70 and 0.78 (values increasing with increasing porosity). Experimental data gives a ratio between 0.44 and 0.54. Besides a breakdown of geometrical optics, the discrepancy may here also be influenced by a difference between intraparticle and interparticle porosity in combination with multiple intraparticle scattering.

To conclude, we have presented an experimental approach for investigation of how light samples pores and solid parts of porous media. It allows nondestructive assessment of porosity and improves fundamental understanding of the interaction of light and porous media. Our observations cannot be fully explained by the utilized two-state model, revealing a need for refined modeling. In addition, our results show that the average refractive index cannot be based on volume fractions only, a complication previously discussed in connection with extremely scattering porous semiconductors [2,19]. Our approach may be used to test refined models. Ultimately, knowledge on how light samples porous media allow improved analysis of signals obtained in e.g., absorption, fluorescence, and Raman spectroscopy of porous media.

References

1. D. S. Wiersma, P. Bartolini, A. Lagendijk, and R. Righini, Nature **390**, 671 (1997).
2. P. M. Johnson, A. Imhof, B. P. J. Bret, J. G. Rivas, and A. Lagendijk, Phys. Rev. E **68**, 016604 (2003).
3. P. Matousek, Chem. Soc. Rev. **36**, 1292 (2007).
4. L. A. Averett and P. R. Griffiths, Appl. Spectrosc. **62**, 377 (2008).
5. Z. Q. Shi and C. A. Anderson, Anal. Chem. **81**, 1389 (2009).
6. J. G. J. Peelen and R. Metselaa, J. Appl. Phys. **45**, 216 (1974).
7. J. Manara, R. Caps, F. Raether, and J. Fricke, Opt. Commun. **168**, 237 (1999).
8. T. Svensson and Z. Shen, Appl. Phys. Lett. **96**, 021107 (2010).
9. C. Toninelli, E. Vekris, G. A. Ozin, S. John, and D. S. Wiersma, Phys. Rev. Lett. **101**, 123901 (2008).
10. A. Wolf, B. Terheiden, and R. Brendel, J. Appl. Phys. **104**, (2008).
11. G. Somesfalean, M. Sjöholm, J. Alnis, C. af Klinteberg, S. Andersson-Engels, and S. Svanberg, Appl. Opt. **41**, 3538 (2002).
12. T. Svensson, M. Andersson, L. Rippe, S. Svanberg, S. Andersson-Engels, J. Johansson, and S. Folestad, Appl. Phys. B **90**, 345 (2008).
13. M. Sjöholm, G. Somesfalean, J. Alnis, S. Andersson-Engels, and S. Svanberg, Opt. Lett. **26**, 16 (2001).
14. T. Svensson, M. Andersson, L. Rippe, J. Johansson, S. Folestad, and S. Andersson-Engels, Opt. Lett. **33**, 80 (2008).
15. E. Alerstam, S. Andersson-Engels, and T. Svensson, Opt. Express **16**, 10440 (2008).
16. T. Svensson, E. Alerstam, D. Khoptyar, J. Johansson, S. Folestad, and S. Andersson-Engels, Rev. Sci. Instrum. **80**, 063105 (2009).
17. A. S. Gittings, R. Bandyopadhyay, and D. J. Durian, Europhys. Lett. **65**, 414 (2004).
18. M. Schmiedeberg, M. F. Miri, and H. Stark, Eur. Phys. J. E **18**, 123 (2005).
19. F. J. P. Schuurmans, D. Vanmaekelbergh, J. van de Lagemaat, and A. Lagendijk, Science **284**, 141 (1999).